Eri silkworm spins mechanically robust silk fibers regardless of reeling speed

Kenjiro Yazawa[1,2]*, *Yuka Tatebayashi*[1], *and Zenta Kajiura*[1]

[1]Department of Applied Biology, Faculty of Textile Science and Technology,
Shinshu University, 3-15-1 Tokida, Ueda City, Nagano 386-8567, Japan

[2]Division of Biological and Medical Fiber, Institute for Fiber Engineering,
Interdisciplinary Cluster for Cutting Edge Research,
Shinshu University, 3-15-1 Tokida, Ueda City, Nagano 386-8567, Japan

Keywords: wild silkworm, domesticated silkworm, eri silkworm, silk fiber, reeling speed, *Samia ricini*,

*Corresponding author: Kenjiro Yazawa

Tel: +81-268-21-5353

E-mail: kenjiro_yazawa@shinshu-u.ac.jp

ABSTRACT

Wild silkworms survive in the environmental habitats in which temperature and humidity vary based on weather. In contrast, domesticated silkworms live in mild environments where temperature and humidity are generally maintained at constant levels. Previous studies showed that the mechanical strengths and molecular orientation of the silk fibers reeled from domesticated silkworms are significantly influenced by the reeling speed. Here we investigated

the effects of the reeling speeds on the mechanical properties of eri silk fibers produced by wild silkworms, *Samia cynthia ricini*, which belong to the family of Saturniidae. We found that the structural, morphological, and mechanical features of eri silk fibers are maintained irrespective of the reeling speed in contrast to those of domesticated silkworm silk fibers. The obtained results are useful not only for understanding the biological basis underlying the natural formation of silk fibers but also for contributing to the design of artificial spinning systems for producing synthetic silk fibers.

INTRODUCTION

Silkworms produce proteinous fibers with biocompatibility and biodegradability. Lightweight and lustrous silk fibers are traditionally used as expensive textile materials with excellent strength and ductility (Omenetto and Kaplan, 2010; Vollrath and Porter, 2009). Hence, in the context of sustainable development goals, silk is regarded as a candidate for promising bio-based fibers (Agnieray et al., 2021). Generally, silk is commercially produced by domesticated silkworms, which have been used for centuries (Ude et al., 2014). Meanwhile, wild silkworm silk fibers are used much less than domesticated silkworm silk fibers because the number of wild silkworms is scarce, and it is difficult to extract silk fibers from the cocoons of wild silkworms due to their mineral reinforcement (Rozet et al., 2019; Rozet and Tamada, 2019; Zhou and Wang, 2020). It has been reported that demineralization using a chelating agent allows the reeling of commercial lengths of wild silk fibers with good quality, which contributes to the development of the wild silk industry (Gheysens et al., 2011).

A lot of attention has been paid to a variety of wild silkworms not only for the production of silk but also for their benefits in structural and medical materials (Kundu et al., 2012). This is not only because wild silkworm silk fibers have their own natural color but also because they often have excellent mechanical properties compared with domesticated silkworm (Guan et al., 2017; Malay et al., 2016). The mechanical properties of silk fibers are largely influenced by their crystal structures (Guo et al., 2017). It is known that the crystal region of silk mainly determines its mechanical strength. However, the amorphous region of silk contributes to its extensibility (Fang et al., 2016). The crystal region of wild silkworm silk consists of polyalanine sequences, which is the case with spider silk (Malay et al., 2016). Meanwhile, the average length of the

polyalanine motifs of wild silkworm silk is often longer than that of spider silk (Numata et al., 2015; Tsubota et al., 2016). In contrast, the crystal region of domesticated silkworm silk has alternative sequences of glycine and alanine (Malay et al., 2016). We have reported that dragline silk fibers, which are used as mechanical lifelines of spiders, maintain their structural and mechanical properties irrespective of the reeling speed during forced spinning (Yazawa and Sasaki, 2021). The mechanically robust nature of spider dragline silk contrasts with the case of domesticated silkworm (*Bombyx mori*) silk fibers. The molecular orientation and mechanical strength of domesticated silkworm silk fibers are known to be significantly influenced by the reeling speed (Du et al., 2006; Khan et al., 2008; Mortimer et al., 2013; Pérez-Rigueiro et al., 2001b; Riekel et al., 2000; Shao and Vollrath, 2002; Wu et al., 2009). Domesticated silkworm silk fibers show higher degrees of orientation and crystallinity with the increase in the reeling speed, enabling the improvement of the tensile strength of silkworm silk. Since wild silkworms need to spin their silk fibers regardless of the weather, it is speculated that the spinning mechanism of silk fibers might differ between wild and domesticated silkworms. In addition, wild silkworms hasten to spin their silk fibers in the case of emergencies, such as abrupt falling and sudden invasion by their predators. Accordingly, we have hypothesized that wild silkworms might have been endowed with a higher level of adaptation against environmental disturbances compared with domesticated silkworms.

To verify the above-mentioned hypothesis, in this study, we used the larvae of an eri-silkmoth, *Samia cynthia ricini*, as a model of wild silkworms, and we forcibly reeled silk fibers from a live wild silkworm. The body size of eri silkworms is the third largest after *Bombyx mori* and tussah, and the lifecycle of eri silkworms is shorter than that of *B. mori*. Meanwhile, the cocoon size of eri silkworms is larger than that of *B. mori*. *B. mori* silkworms can only be fed with mulberry leaves, while eri silkworms can be fed with the leaves of several trees. These features make it easier for eri silkworms to rear. It is known that the fracture surface of wild silkworm silk has a porous structure, which can be a structural defect (Akai, 2005). Therefore, it is also interesting to know how the fracture surface of eri silk fibers changes after forced reeling. Accordingly, we investigated the effects of the reeling speeds on the structural, mechanical, and morphological properties of eri silkworm silk.

MATERIALS AND METHODS

Collection of wild silkworm silk fibers

Eri silk fibers were forcibly collected from wild silkworms, *Samia cynthia ricini* (*S. c. ricini*), which were reared at Shinshu University in Nagano, Japan. Diet can affect the amino acid composition of silk fibers (Cheng et al., 2018; Ito et al., 1995). Accordingly, the eri silkworms used in the experiment were only fed with castor leaves to minimize the effects of dietary conditions. The eri silk fibers were forcibly and directly reeled from the late fifth instar larvae of *S. c. ricini* restrained by two pieces of sponge and fixed with rubber bands (Fig. 1). The forced reeling process was performed in an experimental chamber, where the temperature was set at 25°C and the relative humidity (RH) was set at 40%. The eri silk fibers were reeled onto a spool that was rotated by a motorized apparatus (Harada Corp., Nagano, Japan). The reeling speeds were set at the following constant values: 3, 15, 30, 45, 60, and 75 mm s^{-1}, covering most of the natural spinning speeds of silkworms (Miura et al., 1993). For each speed, the silk samples from the start and end of reeling were avoided. All the collected silk fibers were left to dry in lightproof boxes with silica gel to minimize the structural change of silk fibers derived from the variation of the extrinsic factors (Boulet-Audet et al., 2016; Yazawa et al., 2020). After the forced reeling process, the wild silkworms produced cocoons.

Fourier-transform infrared (FT-IR) spectroscopy

A FT-IR device (IR Prestige-21, Shimadzu Corp., Kyoto, Japan) equipped with an attenuated total reflectance accessory (DuraSamplIR; Smith Detection, London, England) was used to examine the peaks derived from the secondary structures of the eri silk fibers. For each measurement, 128 scans were accumulated with a resolution of 4 cm^{-1} at 25°C under an RH ranging from 35% to 45%.

Wide-angle X-ray scattering (WAXS)

A synchrotron WAXS measurement was performed on bundles of eri silk fibers using X-ray energy of 12.4 keV (wavelength: 0.1 nm) at the BL-10C beamline of Photon Factory, Tsukuba, Japan (Shimizu et al., 2019). The sample-to-detector distance for the WAXS measurement was 238 mm, and the exposure time for each scattering pattern was 10 s at 25°C

under an RH ranging from 30% to 40%. The obtained scattering data were converted into one-dimensional and radially integrated profiles using the Fit2D software (Hammersley et al., 1996). The data were corrected for background scattering. Also, the crystallinity was calculated by dividing the areas of the crystal peaks by the total area of the crystal peaks and amorphous halo by fitting the Gaussian function using Igor Pro 8.03 (WaveMetrics, Inc., Portland, OR). Moreover, according to previous procedures, the degree of orientation was evaluated from the (210) peak representing the crystalline β-sheet structure based on the full width at half maximum (FWHM) value (Malay et al., 2016; Yazawa et al., 2020).

Tensile test

The eri silk single fiber obtained by forced reeling was subjected to tensile tests using a test apparatus (RTC-1250A, A&D Company Ltd., Tokyo, Japan) at 25°C under an RH ranging from 35% to 40%. The initial length of the eri silk single fiber was set at 5 mm, and the deformation rate was set at 10 mm min^{-1} using a load cell with 1 N. The silk fiber was carefully fixed with the same force each time. The fracture surface and diameters of the tensile test specimens of the eri silk fibers were individually examined by SEM. The cross-sectional areas of the tensile test specimen of the eri silk fibers were individually evaluated by tracing the edge contours of the silk fibers. Twenty samples per silking speed of the eri silk fibers were tested. All data were processed in Microsoft Excel by excluding the slack regions from the initial stages of the tensile tests. The tensile strength, elongation at break, Young's modulus, and toughness were evaluated based on the resultant stress–strain curves.

Scanning electron microscopy (SEM)

The fracture surface, side-view morphology, and diameters of the tensile test specimens of the eri silk fibers were individually examined by SEM (SU1510, Hitachi High-Tech Corporation, Tokyo, Japan) at 25°C. The eri silk fibers were mounted on an aluminum stub with a conductive tape and then sputter-coated with gold for 1 min using a smart coater (JEOL, Tokyo, Japan) prior to SEM visualization at 15 kV. The cross-sectional area of the individual tensile test specimen of the eri silk fibers was evaluated by tracing the edge contours of the silk fibers using ImageJ (NIH, Bethesda, MD, USA).

Statistical analysis

A statistical analysis was performed by Student's *t*-test using Microsoft Excel to determine if the averages are significantly different. The differences were considered significant when the *p*-values were less than 0.05.

RESULTS

FT-IR and WAXS measurements of eri silk fibers obtained by forced reeling under different reeling speeds

FT-IR spectroscopy has been applied to evaluate the bending vibrations and stretching associated with amide bonds originating from secondary structures of eri silkworm silk fibers. Meanwhile, WAXS measurement can detect the coherent interference of scattered X-rays passing through the crystal (Fig. 2), enabling to monitor the crystal regions of eri silkworm silk fibers. Therefore, the protein secondary structure of the eri silkworm silk fiber was monitored by FT-IR, while the crystallinity was evaluated by the WAXS data. Forced reeling of eri silk fibers was performed at different reeling speeds. The obtained eri silk fibers were examined by FT-IR to analyze the secondary structures of the silk fibers (Fig. 3a). A peak centered at 1625 cm^{-1} indicates the presence of crystalline β-sheets in the eri silk fibers (Moseti et al., 2019a; Moseti et al., 2019b). The FT-IR spectra of the eri silk fibers displayed no observable peak shifts based on the reeling speed (Fig. S1). The crystallinity and degree of molecular orientation were examined based on the WAXS data. Two-dimensional WAXS images of the eri silk fibers (Fig. 2) were converted into one-dimensional plots using radial integration (Fig. 3b). The (210) and (020) peaks were detected in the one-dimensional WAXS profiles, indicating the formation of a crystalline β-sheet structure (Moseti et al., 2019a; Moseti et al., 2019b). Based on the WAXS profiles, the positions of the peaks originating from the crystalline β-sheets were maintained regardless of the reeling speeds (Fig. 3b). Thus, the crystal structure of the eri silk fibers did not change. Small peaks in 3, 30, 45, and 60 mm/s of WAXS data were derived from calcium oxalate that covers the cocoons of wild silkworms (Gheysens et al., 2011).

The one-dimensional WAXS plot was deconvoluted into crystal and amorphous fractions using Gaussian functions to examine the crystallinity of the eri silk fibers (Fig. S2), which was maintained irrespective of the reeling speed (Fig. 4a). The effects of the reeling speeds on the molecular orientation degree were also analyzed based on the FWHM values that were calculated by the azimuthal integration of the (210) peak in the two-dimensional WAXS profiles (Fig. 4b). The FWHM values did not significantly change with the different reeling speeds. These results indicate that the crystal structure and molecular alignment of the forcibly reeled eri silk fibers were not influenced by the reeling speed. Furthermore, the diameters of the eri silk fibers were evaluated by SEM measurements (Fig. 4c). The results showed that the diameters of the eri silk fibers were not affected by the reeling speed.

Mechanical characterization of the eri silk fibers obtained by forced reeling under different reeling speeds

The structural features of the eri silk fibers were not influenced by the reeling speeds. Next, the effects of the reeling speeds on the mechanical parameters of the eri silk fibers were examined through tensile testing. The eri silk fibers presented tensile strength values ranging from 0.15 GPa to 0.20 GPa and extensibility values ranging from 15% to 35% under the used reeling speeds in this study (Fig. 5). These tensile strength and extensibility values are within the range of naturally spun eri silk fibers (Malay et al., 2016). Thus, the stress–strain curves of the eri silk fibers were not significantly influenced by the reeling speeds. Then, the tensile strength, elongation at break, Young's modulus, and toughness of the eri silk fibers were summarized, as shown in Fig. 6, based on the stress–strain curves. The changes in the mechanical parameters were negligible for the given reeling speeds.

SEM visualization of the eri silk fibers obtained by forced reeling under different reeling speeds

The morphological features of the eri silk fibers obtained by forced reeling under different reeling speeds were visualized by SEM imaging, as shown in Fig. 7. Eri silk fibers comprise a semicrystalline fibroin core and an outer layer of sericin. The surface of the eri silk fibers was smooth regardless of the reeling speed. On the other hand, the fracture surface of the naturally spun eri silkworm silk fibers had voids (Fig. S3). Furthermore, the diameter of the silk samples

from the start of reeling tended to increase (Fig. S4). In addition, smaller diameters and cracks were detected in the eri silk samples from the end of forced reeling for producing a continuous thread of several hundred meters long (Fig. S5), probably originating from the lack of protein solution in the spinning dope or from the defects of the sericin layers formed during the silk fiber formation. These morphological features suggest that wild silkworm *S. c. ricini* spin silk fibers with a constant diameter irrespective of the reeling speed.

DISCUSSION

The effects of the reeling speeds on the structural and mechanical properties of the forcibly spun silk fibers were examined using *S. c. ricini* as a model of Saturniidae wild silkworms. The crystal structure, surface morphology, and mechanical parameters of the eri silk fibers were not significantly changed by the reeling speeds. The obtained results agree with those of the previous study, in which forced reeling of dragline silk fibers from the web-building spider *Trichonephila clavata* was performed at different reeling speeds (Yazawa and Sasaki, 2021). Dragline silk fibers ensure robustness irrespective of the spinning speed. Day and night, the insects and animals living in the wild should adapt to environmental changes. It has been reported that the physical properties of domesticated silkworm cocoons are influenced by environmental temperature, wind speed, and humidity. Environmental temperature affects the speed of the figure-of-eight movement of domesticated silkworms and changes the morphological properties of cocoons (Offord et al., 2016). Moreover, humidity conditions vary the speed of the water removal from newly spun silk fibers, which influences the crystallization behavior (Boulet-Audet et al., 2016), and wind loading might affect the spinning speed of silkworms (Vollrath et al., 2001). Such environmental disturbances might also change the physical properties of the silk fibers produced by wild insects and animals. Accordingly, it is essential for insects and animals in their natural habitats to maintain the mechanical toughness of their silk fibers. Pérez-Rigueiro et al. have demonstrated a strong correlation between the silking force and tensile behavior of spider silk (Pérez-Rigueiro et al., 2001a; Perez-Rigueiro et al., 2005). They found that the silk fibers spun at high silking force are stiff, while the silk fibers spun at low silking force are extensible. Considering that eri silkworms produced structurally and mechanically robust silk fibers in this study, eri silkworms might add a particular level of tensile load to their silk fibers by

adjusting their ventral and dorsal muscles near the spinneret. To reveal the details of the muscle manipulation, we are now investigating the electric potential that is exerted near the spinneret of wild silkworms and spiders during forced silking to compare it with the electric potential exerted by domesticated silkworms. It should be noted that the variation in physical properties between eri silkworm and *B. mori* silk fibers might be derived from different genus and species. Further study should be needed using other species of wild silkworms to elucidate the influence of genus.

Akai et al. reported that the fracture surfaces of wild silkworm silk fibers have abundant voids (Akai, 2005). These voids are thought to be derived from the lysosomes in silk glands and to play an important role in maintaining certain temperature and humidity values inside cocoons. Meanwhile, such voids can be structural defects and can result in weaker mechanical strengths. In contrast, after forced reeling, the fracture surfaces of eri silk fibers were visualized by SEM in Fig. 8 and Fig. S6. The fracture surfaces of eri silk fibers displayed dense structures without voids. Thus, forced spinning is useful in decreasing the structural defects of silk fibers and in contributing to the production of mechanically tough silk fibers.

CONCLUSIONS

The effects of various reeling speeds on the structural, morphological, and mechanical properties of forcibly spun silk fibers were analyzed using *S. c. ricini* as a model of wild silkworms. The crystal structures and mechanical properties of the obtained eri silk fibers were not significantly changed by the reeling speed. In addition, the morphological aspects of the eri silk fibers demonstrated fixed diameters and flawless surfaces although the diameter tended to decrease, and the cracks of the surface layers were detected at the end of the forced reeling process. These results indicate that *S. c. ricini* silkworms have evolved to spin silk fibers with a particular level of mechanical toughness so that they can be used as protective shells for their pupae. Wild silkworms might exert a constant tensile force by adjusting the ventral and dorsal muscles near their spinnerets, enabling them to spin mechanically robust silk fibers. This indicates that the insects and animals living in the wild have evolved to spin silk fibers with robustness to the reeling speed. Overall, the results of the forcibly spun wild silkworm silk fibers in this work can help in understanding the natural spinning mechanism of silkworms and in paving the way to determining the best spinning conditions for synthesizing artificial silk fibers

with comparable mechanical properties to those of their natural counterparts. We are now developing an automated rearing system of silkworms from eggs to cocoons in germ-free conditions for the bulk-scale production of silk fibers. Since eri silkworms are resistant to reeling speeds in comparison with domesticated silkworms, eri silkworms can be promising candidates for producing silk fibers using the automated rearing system.

Supplementary Information

Supplementary Information to this article can be found online at xx.

Acknowledgments

This work was financially supported by JSPS Grant-in-Aid for Scientific Research (C) Grant No. 21K12305. The WAXS measurement was performed under the approval of the Photon Factory Program Advisory Committee (Proposal No. 2021G006).

CRediT authorship contribution statement

Kenjiro Yazawa: Conceptualization, Methodology, Validation, Formal analysis, Investigation, Writing - Original Draft, Supervision, Funding acquisition. **Yuka Tatebayashi:** Methodology, Formal analysis, Investigation. **Zenta Kajiura:** Methodology, Investigation.

Declaration of interests

The authors declare that they have no known competing financial interests or personal relationships that could have appeared to influence the work reported in this paper.

References

Agnieray, H., Glasson, J. L., Chen, Q., Kaur, M. and Domigan, L. J. (2021). Recent developments in sustainably sourced protein-based biomaterials. *Biochem. Soc. Trans.* **49**, 953-964.

Akai, H. (2005). Porous cocoon filaments: Their characteristics and formation. *Int. J. wild silkmoth & silk* **10**, 57-74.

Boulet-Audet, M., Holland, C., Gheysens, T. and Vollrath, F. (2016). Dry-spun silk produces native-like fibroin solutions. *Biomacromolecules* **17**, 3198-3204.

Cheng, L., Huang, H., Zeng, J., Liu, Z., Tong, X., Li, Z., Zhao, H. and Dai, F. (2018). Effect of different additives in diets on secondary structure, thermal and mechanical properties of silkworm silk. *Materials* **12**, 14.

Du, N., Liu, X. Y., Narayanan, J., Li, L., Lim, M. L. M. and Li, D. (2006). Design of superior spider silk: From nanostructure to mechanical properties. *Biophys. J.* **91**, 4528-4535.

Fang, G. Q., Huang, Y. F., Tang, Y. Z., Qi, Z. M., Yao, J., Shao, Z. Z. and Chen, X. (2016). Insights into silk formation process: Correlation of mechanical properties and structural evolution during artificial spinning of silk fibers. *Acs Biomater. Sci. Eng.* **2**, 1992-2000.

Gheysens, T., Collins, A., Raina, S., Vollrath, F. and Knight, D. P. (2011). Demineralization enables reeling of wild silkmoth cocoons. *Biomacromolecules* **12**, 2257-2266.

Guan, J., Zhu, W., Liu, B., Yang, K., Vollrath, F. and Xu, J. (2017). Comparing the microstructure and mechanical properties of *Bombyx mori* and *Antheraea pernyi* cocoon composites. *Acta Biomater.* **47**, 60-70.

Guo, C. C., Zhang, J., Wang, X. G., Nguyen, A. T., Liu, X. Y. and Kaplan, D. L. (2017). Comparative study of strain-dependent structural changes of silkworm silks: Insight into the structural origin of strain-stiffening. *Small* **13**, 1702266.

Hammersley, A. P., Svensson, S. O., Hanfland, M., Fitch, A. N. and Hausermann, D. (1996). Two-dimensional detector software: From real detector to idealised image or two-theta scan. *High Press. Res.* **14**, 235-248.

Ito, H., Muraoka, Y., Yamazaki, T., Imamura, T., Mori, H., Ichida, M., Sumida, M. and Matsubara, F. (1995). Structure and chemical composition of silk proteins in relation to silkworm diet. *Text. Res. J.* **65**, 755-759.

Khan, M. M. R., Morikawa, H., Gotoh, Y., Miura, M., Ming, Z., Sato, Y. and Iwasa, M. (2008). Structural characteristics and properties of *Bombyx mori* silk fiber obtained by different artificial forcibly silking speeds. *Int. J. Biol. Macromol.* **42**, 264-270.

Kundu, S. C., Kundu, B., Talukdar, S., Bano, S., Nayak, S., Kundu, J., Mandal, B. B., Bhardwaj, N., Botlagunta, M., Dash, B. C. et al. (2012). Nonmulberry silk biopolymers. *Biopolymers* **97**, 455-467.

Malay, A. D., Sato, R., Yazawa, K., Watanabe, H., Ifuku, N., Masunaga, H., Hikima, T., Guan, J., Mandal, B. B., Damrongsakkul, S. et al. (2016). Relationships between physical properties and sequence in silkworm silks. *Sci. Rep.* **6**, 27573.

Miura, M., Takahashi, E., Sugiyama, H. and Morikawa, H. (1993). A Method for measuring the spinning speed of silkworms. *J. Seric. Sci. Jpn.* **62**, 382-391.

Mortimer, B., Holland, C. and Vollrath, F. (2013). Forced reeling of *Bombyx mori* silk: separating behavior and processing conditions. *Biomacromolecules* **14**, 3653-3659.

Moseti, K. O., Yoshioka, T., Kameda, T. and Nakazawa, Y. (2019a). Aggregation state of residual α-helices and their influence on physical properties of *S. c. ricini* native fiber. *Molecules* **24**, 3741.

Moseti, K. O., Yoshioka, T., Kameda, T. and Nakazawa, Y. (2019b). Structure water-solubility relationship in α-helix-rich films cast from aqueous and 1,1,1,3,3,3-hexafluoro-2-propanol solutions of *S. c. ricini* silk fibroin. *Molecules* **24**, 3945.

Numata, K., Sato, R., Yazawa, K., Hikima, T. and Masunaga, H. (2015). Crystal structure and physical properties of *Antheraea yamamai* silk fibers: Long poly(alanine) sequences are partially in the crystalline region. *Polymer* **77**, 87-94.

Offord, C., Vollrath, F. and Holland, C. (2016). Environmental effects on the construction and physical properties of *Bombyx mori* cocoons. *J. Mater. Sci.* **51**, 10863-10872.

Omenetto, F. G. and Kaplan, D. L. (2010). New opportunities for an ancient material. *Science* **329**, 528-531.

Pérez-Rigueiro, J., Elices, M., Llorca, J. and Viney, C. (2001a). Tensile properties of *Argiope trifasciata* drag line silk obtained from the spider's web. *J. Appl. Polym. Sci.* **82**, 2245-2251.
Pérez-Rigueiro, J., Elices, M., Llorca, J. and Viney, C. (2001b). Tensile properties of silkworm silk obtained by forced silking. *J. Appl. Polym. Sci.* **82**, 1928-1935.
Perez-Rigueiro, J., Elices, M., Plaza, G., Real, J. I. and Guinea, G. V. (2005). The effect of spinning forces on spider silk properties. *J. Exp. Biol.* **208**, 2633-2639.
Riekel, C., Madsen, B., Knight, D. and Vollrath, F. (2000). X-ray diffraction on spider silk during controlled extrusion under a synchrotron radiation X-ray beam. *Biomacromolecules* **1**, 622-626.
Rozet, S., Kobayashi, H., Kajiura, Z. and Tamada, Y. (2019). Characterization of *Antheraea pernyi* fibroin films from the aqueous solution prepared by an improved process. *J. Silk Sci. Tech. Jpn.* **27**, 33-42.
Rozet, S. and Tamada, Y. (2019). An improved process for stably preparing of *Antheraea pernyi* fibroin aqueous solution. *J. Silk Sci. Tech. Jpn.* **27**, 23-31.
Shao, Z. and Vollrath, F. (2002). Materials: Surprising strength of silkworm silk. *Nature* **418**, 741-741.
Shimizu, N., Mori, T., Nagatani, Y., Ohta, H., Saijo, S., Takagi, H., Takahashi, M., Yatabe, K., Kosuge, T. and Igarashi, N. (2019). BL-10C, the small-angle X-ray scattering beamline at the photon factory. *AIP Conf. Proc.* **2054**, 060041.
Tsubota, T., Yamamoto, K., Mita, K. and Sezutsu, H. (2016). Gene expression analysis in the larval silk gland of the eri silkworm *Samia ricini*. *Insect Sci.* **23**, 791-804.
Ude, A. U., Eshkoor, R. A., Zulkifili, R., Ariffin, A. K., Dzuraidah, A. W. and Azhari, C. H. (2014). *Bombyx mori* silk fibre and its composite: A review of contemporary developments. *Mater. Des.* **57**, 298-305.
Vollrath, F., Madsen, B. and Shao, Z. Z. (2001). The effect of spinning conditions on the mechanics of a spider's dragline silk. *Proc. Royal Soc. B* **268**, 2339-2346.
Vollrath, F. and Porter, D. (2009). Silks as ancient models for modern polymers. *Polymer* **50**, 5623-5632.
Wu, X., Liu, X.-Y., Du, N., Xu, G. and Li, B. (2009). Unraveled mechanism in silk engineering: Fast reeling induced silk toughening. *Appl. Phys. Lett.* **95**, 093703.
Yazawa, K., Malay, A. D., Masunaga, H., Norma-Rashid, Y. and Numata, K. (2020). Simultaneous effect of strain rate and humidity on the structure and mechanical behavior of spider silk. *Commun. Mater.* **1**, 10.
Yazawa, K. and Sasaki, U. (2021). Forcibly spun dragline silk fibers from web-building spider *Trichonephila clavata* ensure robustness irrespective of spinning speed and humidity. *Int. J. Biol. Macromol.* **168**, 550-557.
Zhou, B. and Wang, H. (2020). Structure and functions of cocoons constructed by eri silkworm. *Polymers* **12**, 2701.

Figures

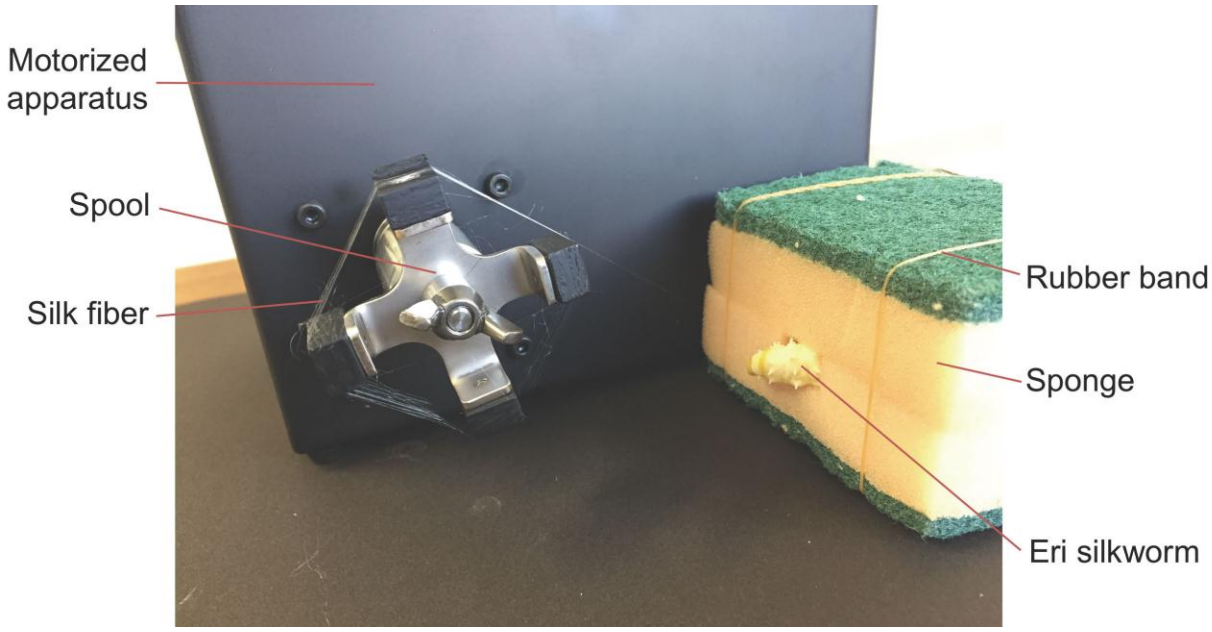

Fig. 1. Picture of silk reeling process from eri silkworm.

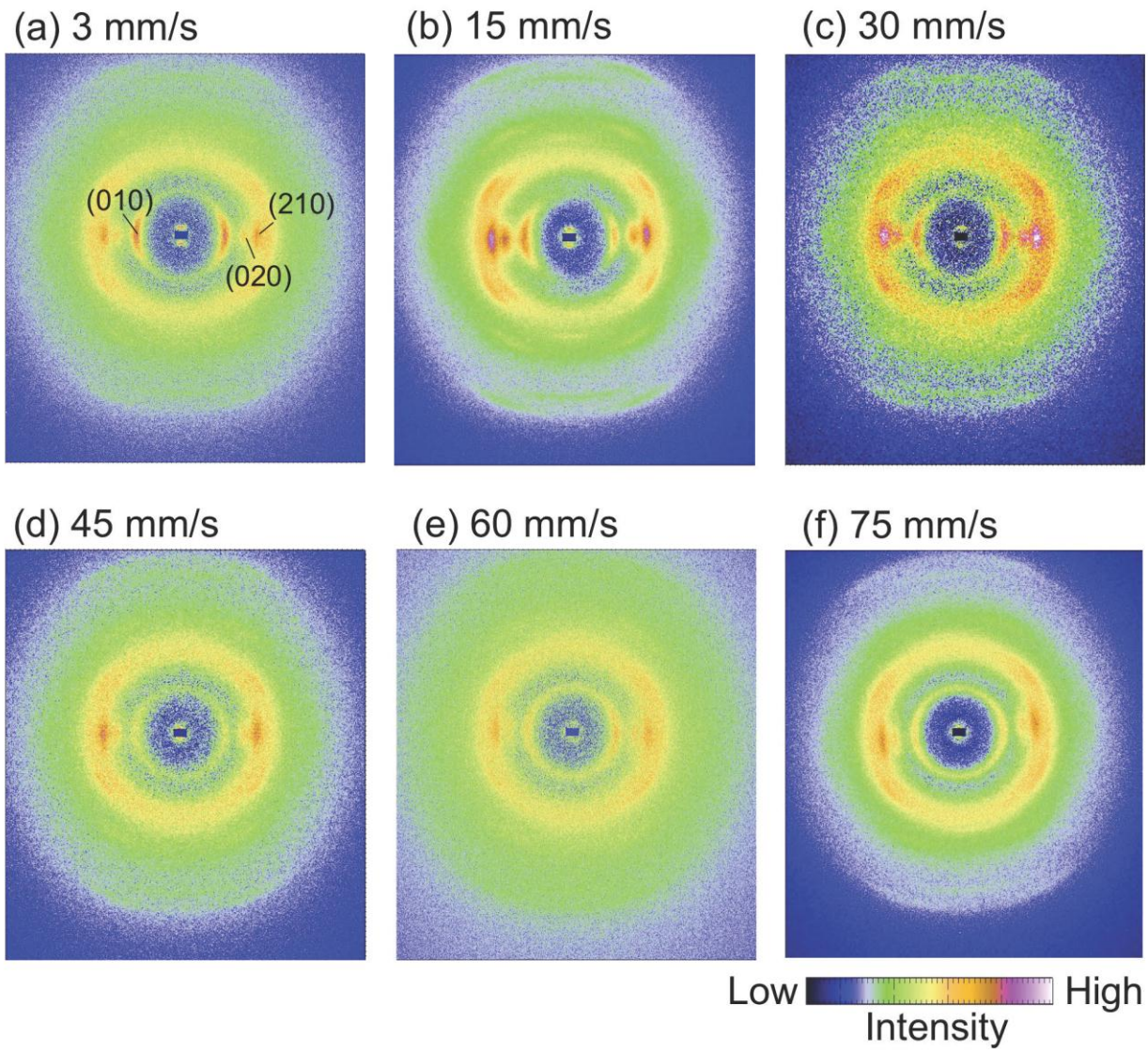

Fig. 2. Two-dimensional WAXS profiles of the eri silkworm silk fibers obtained by forced spinning at different reeling speeds.

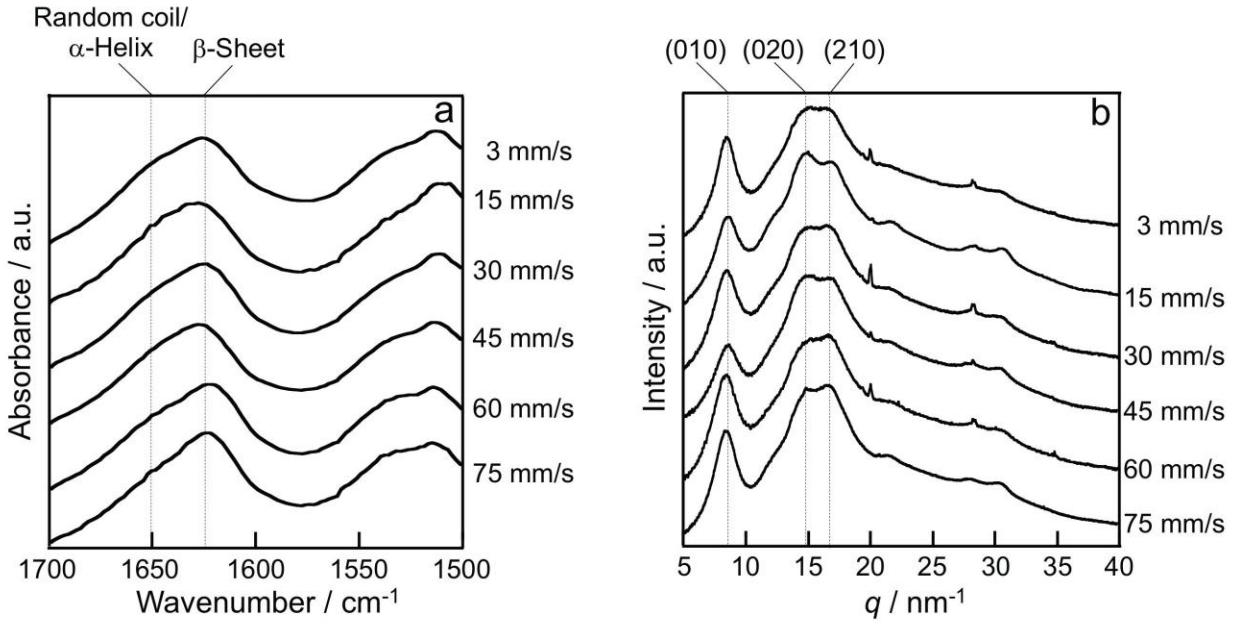

Fig. 3. Structural analysis of the wild silkworm silk fibers obtained at different reeling speeds: (a) amide I region of the FT-IR spectra and (b) one-dimensional, radially integrated WAXS profile. The crystal structure of the eri silkworm silk fibers was maintained despite varying reeling speeds.

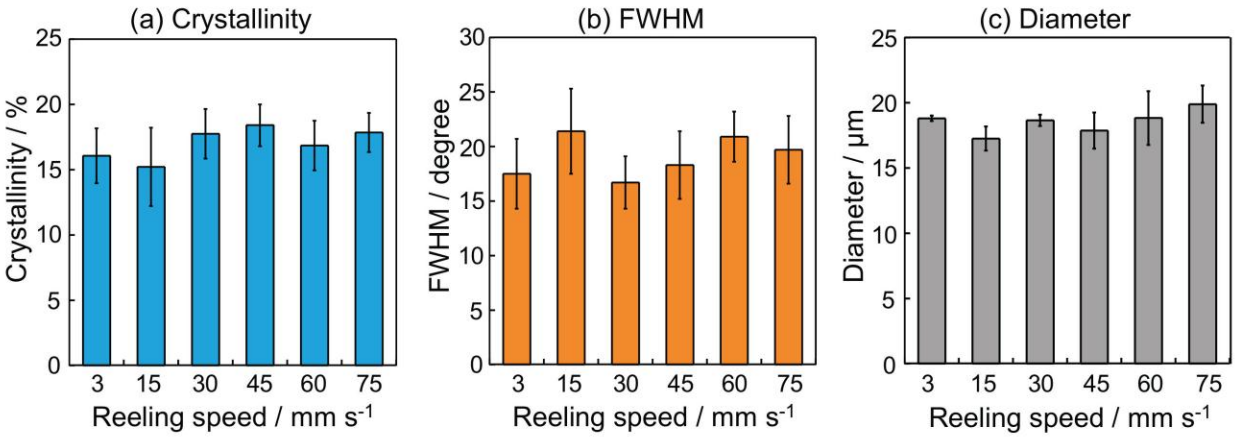

Fig. 4. Structural and morphological analyses of the eri silkworm silk fibers obtained by forced reeling: effects of the reeling speed and humidity on (a) crystallinity, (b) the full width at half maximum (FWHM) of the (210) peak, and (c) fiber diameter. The error bars represent the standard deviations (n = 5). The crystal structure and diameter of the eri silkworm silk fibers were maintained despite varying reeling speeds.

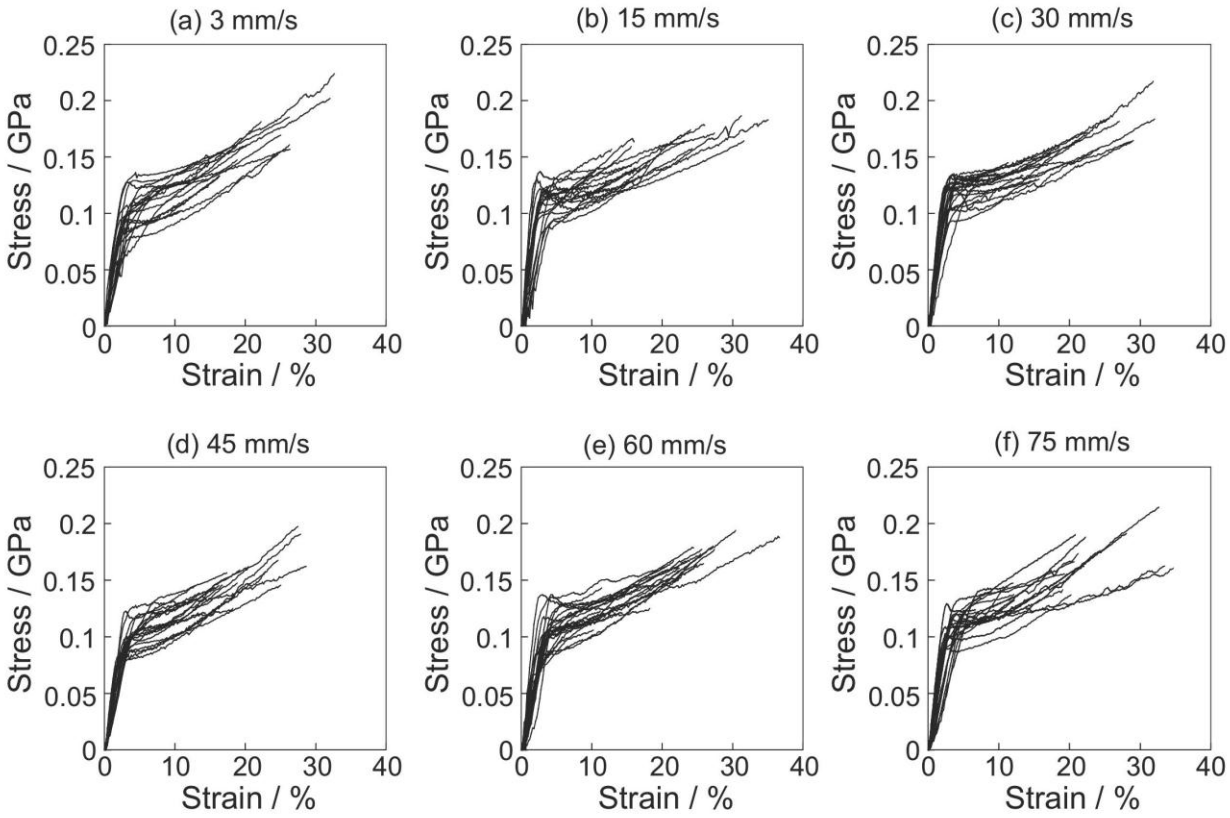

Fig. 5. Stress–strain curves of the eri silkworm silk fibers obtained by forced reeling at different reeling speeds (n = 20). The stress–strain curves of the eri silkworm silk fibers displayed similar behaviors despite varying reeling speeds.

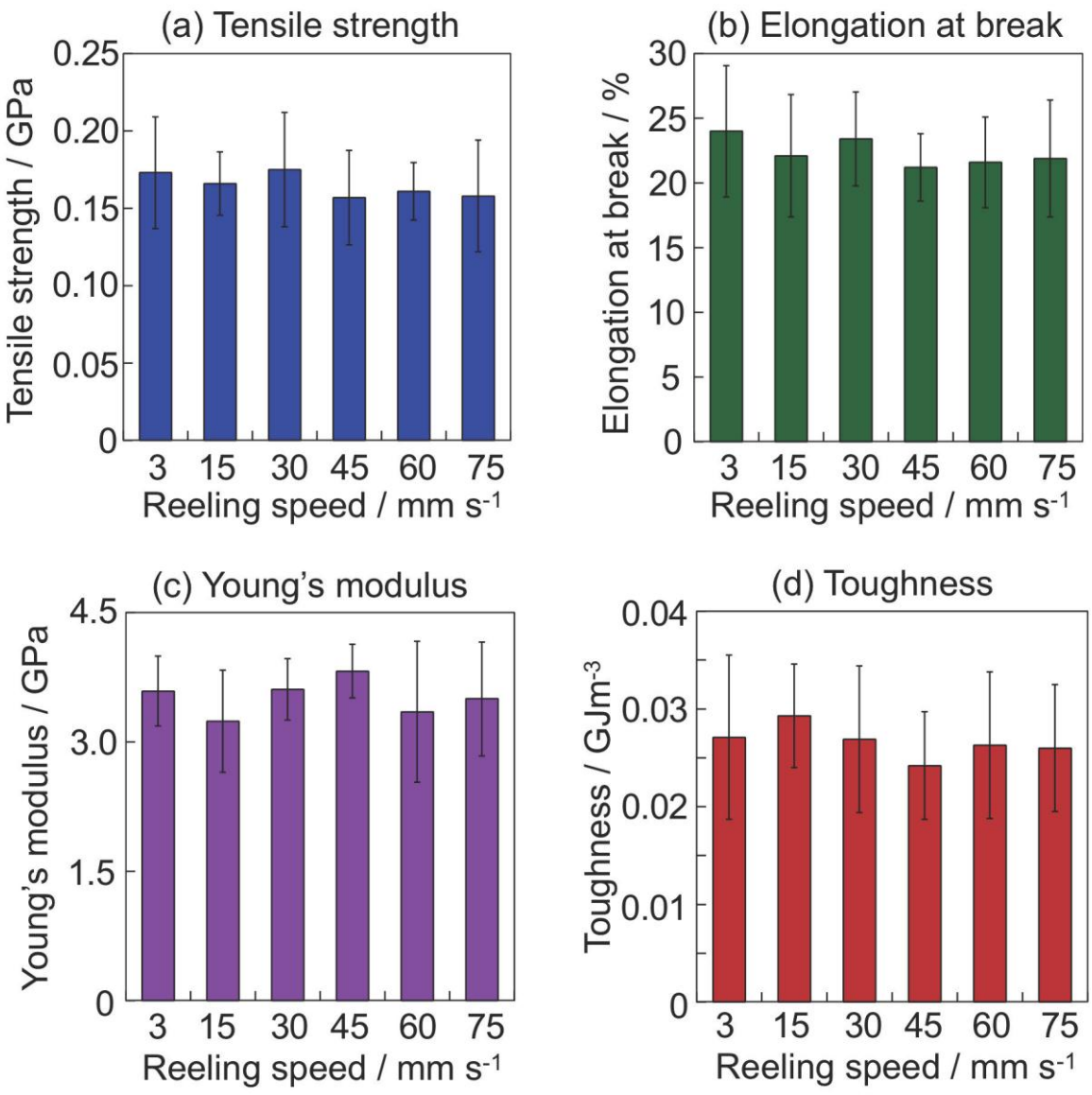

Fig. 6. Mechanical parameters of the eri silkworm silk fibers obtained by forced reeling at different reeling speeds: (a) tensile strength, (b) elongation at break, (c) Young's modulus, and (d) toughness. The error bars represent the standard deviations (n = 20). The mechanical parameters of the eri silkworm silk fibers were not significantly changed irrespective of the reeling speeds.

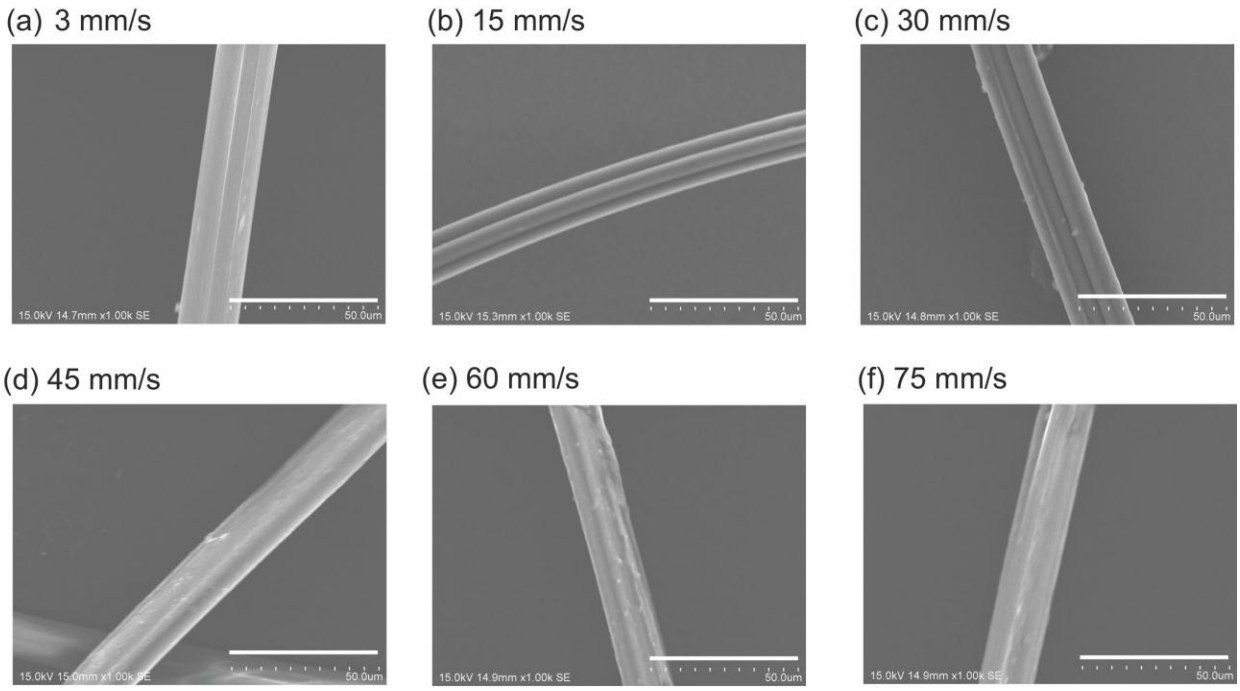

Fig. 7. SEM images of the wild silkworm silk fibers obtained by forced reeling at different reeling speeds. The scale bars denote 50 μm. The morphological aspects of the eri silkworm silk fibers demonstrated morphologically robust features despite varying reeling speeds.

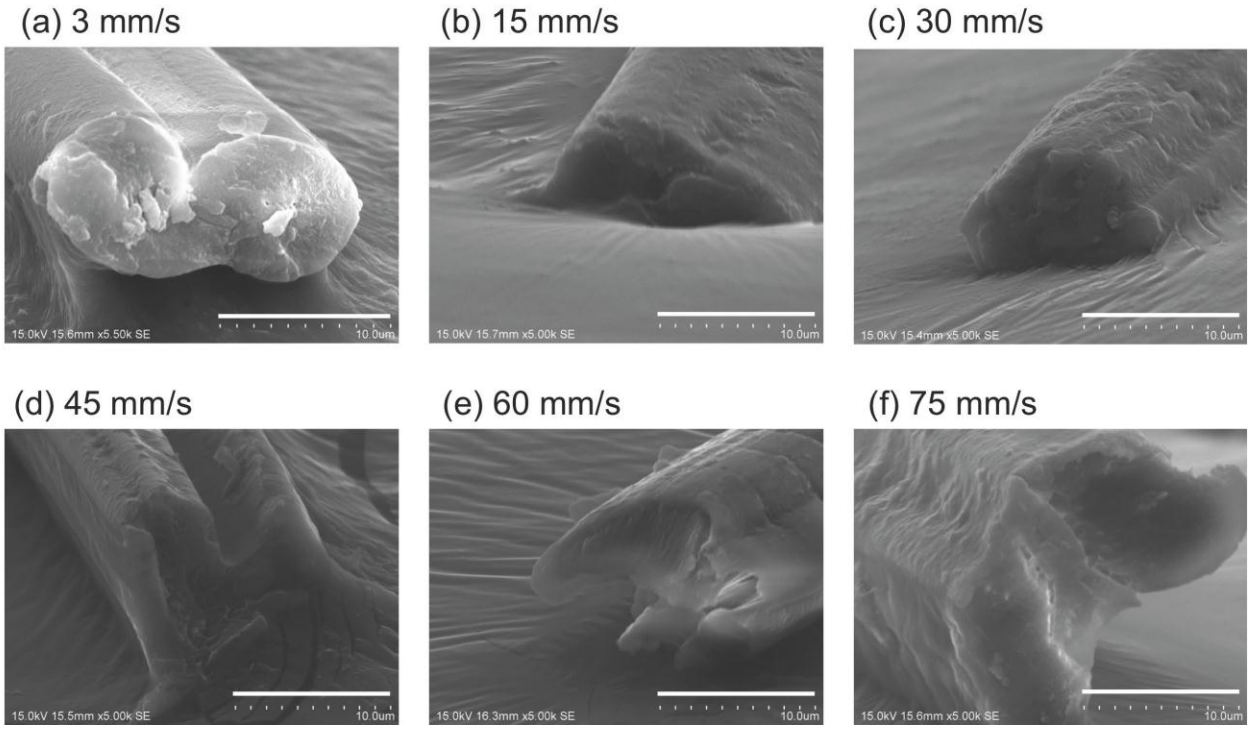

Fig. 8. SEM images showing the fracture surfaces of the tensile test specimens of the eri silkworm silk fibers obtained by forced reeling at different reeling speeds. The scale bars denote 10 μm. The fracture surfaces of the eri silkworm silk fibers obtained by forced reeling demonstrated dense morphology without voids.

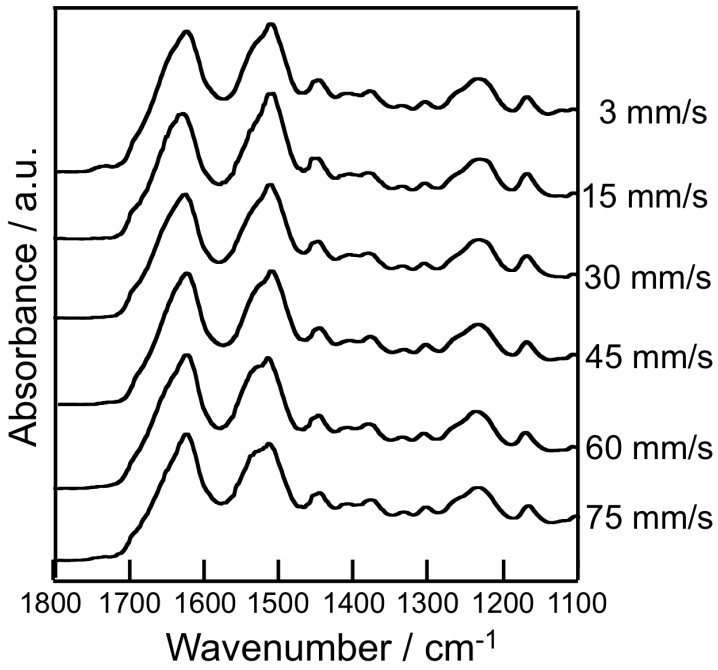

Fig. S1. FT-IR spectra of eri silkworm silk fibers obtained by forced reeling at different reeling speeds.

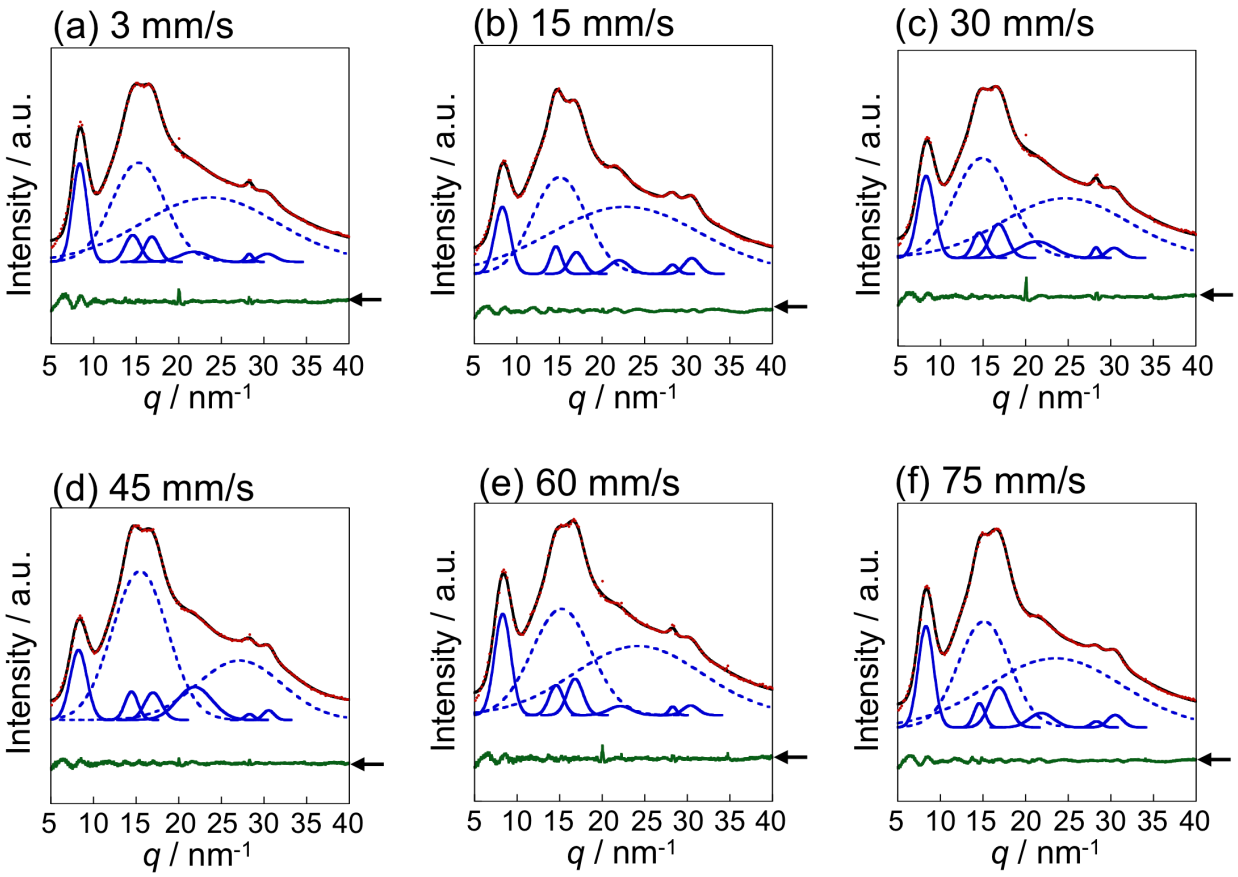

Fig. S2. Peak separations of one-dimensional radial integration WAXS profiles using Gaussian functions for the eri silkworm silk fibers obtained by forced spinning at different reeling speeds. Black lines are fitted curves and broken lines represent the amorphous halos. Solid lines represent the crystal peaks. Arrows show the residual between the fitted curves and the measured curves.

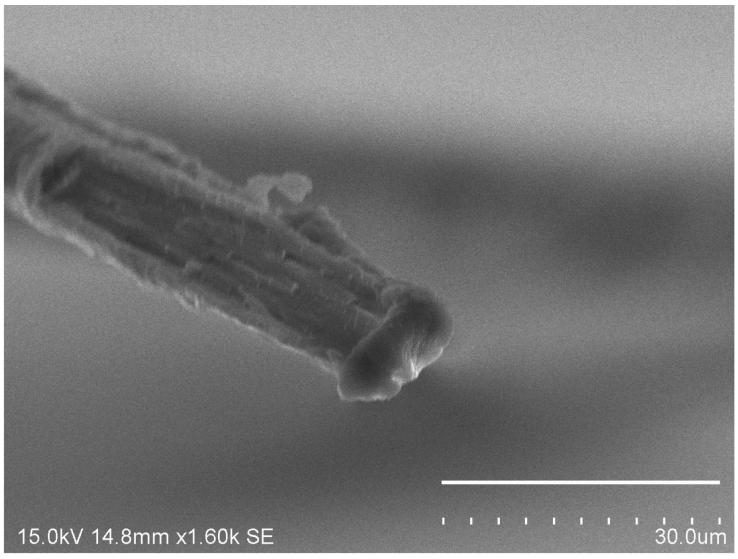

Fig. S3. SEM image showing the fracture surface of the naturally spun eri silkworm silk fibers. Scale bars denote 30 μm.

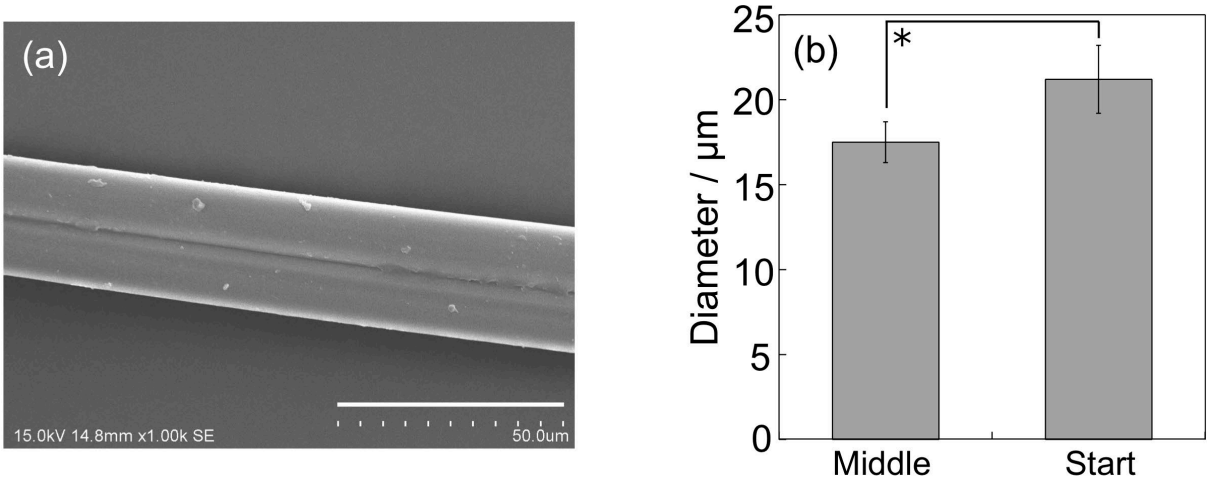

Fig. S4. Morphological feature of the eri silkworm silk fibers obtained from the start of the forced reeling. (a) SEM images of the eri silkworm silk fibers from the start of the forced reeling at 15 mm/s. Scale bars denote 50 μm. (b) Comparison of the fiber diameter at the middle and start of the forced reeling process at 15 mm/s. *Significant differences between groups at $p < 0.05$.

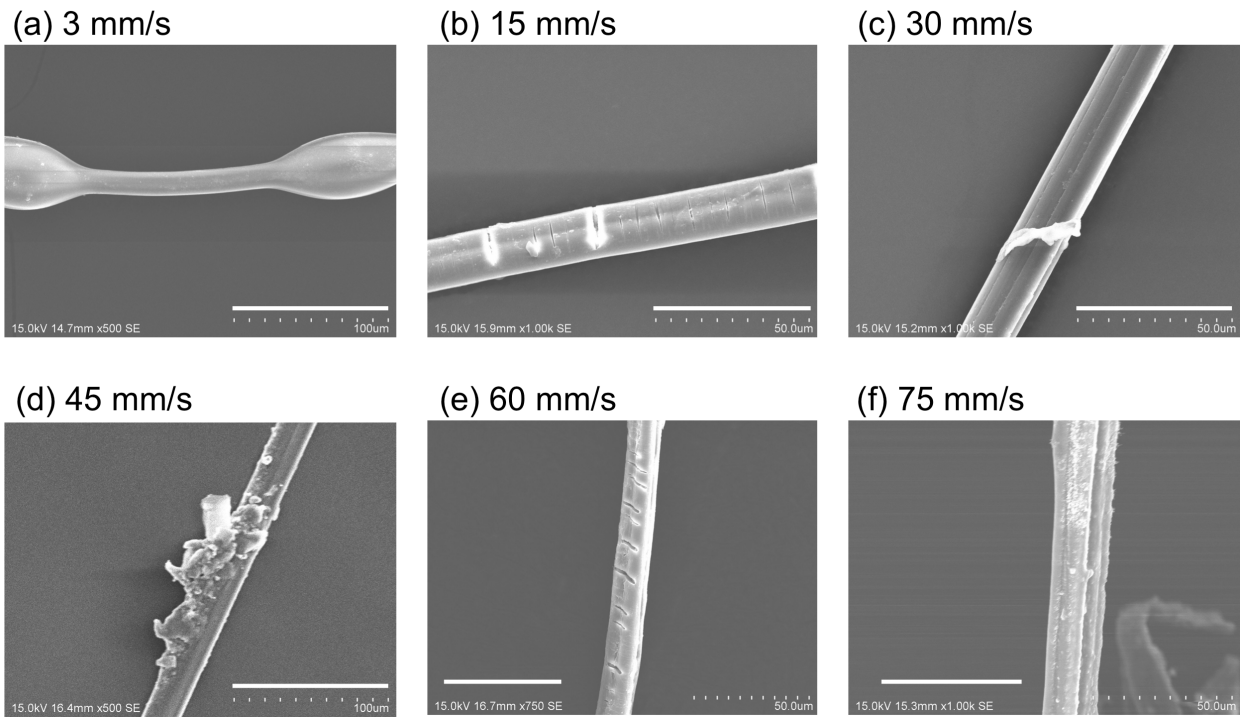

Fig. S5. SEM images of the eri silkworm silk fibers obtained from the end of the forced reeling at different reeling speeds. Scale bars denote 100 μm (a, d) and 50 μm (b, c, e, f).

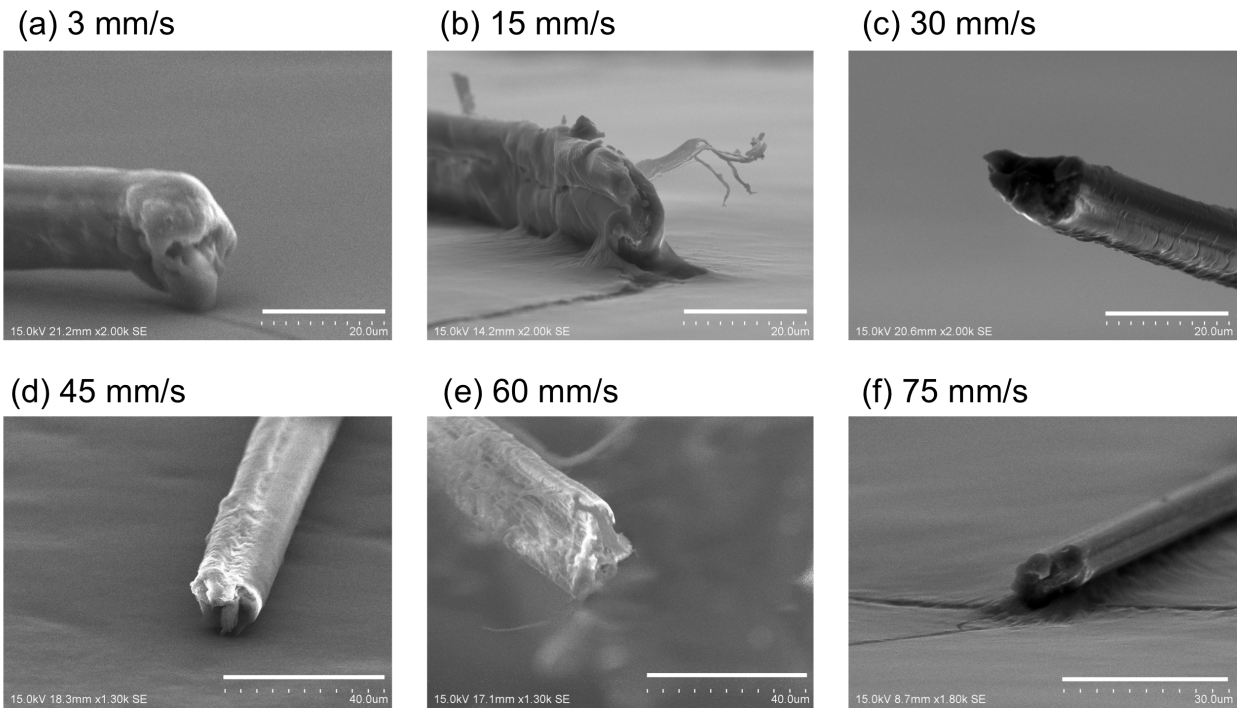

Fig. S6. SEM images showing a fracture surface of the eri silkworm silk fibers obtained by forced spinning at different reeling speeds. Scale bars denote 20 μm (a, b, c), 40 μm (d, e), and 30 μm (f).